Kelpwatch: A new visualization and analysis tool to explore kelp canopy dynamics reveals variable resistance and resilience to marine heat waves

Tom W. Bell[1*], Kyle C. Cavanaugh[2], Vienna R. Saccomanno[3], Katherine C. Cavanaugh[2], Henry F. Houskeeper[2], Norah Eddy[3], Falk Schuetzenmeister[3], Nathaniel Rindlaub[3], Mary Gleason[3]

[1] Department of Applied Ocean Physics and Engineering, Woods Hole Oceanographic Institution, Woods Hole, Massachusetts, United States of America

[2] Department of Geography, University of California Los Angeles, CA, United States of America

[3] The Nature Conservancy, 830 S St., Sacramento, CA, United States of America

* Corresponding author

Email: tbell@whoi.edu

Abstract

Giant kelp and bull kelp forests are increasingly at risk from marine heatwave events, herbivore outbreaks, and the loss or alterations in the behavior of key herbivore predators. The dynamic floating canopy of these kelps is well-suited to study via satellite imagery, which provides high temporal and spatial resolution data of floating kelp canopy across the western United States and Mexico. However, the size and complexity of the satellite image dataset has made ecological analysis difficult for scientists and managers. To increase accessibility of this rich dataset, we created Kelpwatch, a web-based visualization and analysis tool. This tool allows researchers and managers to quantify kelp forest change in response to disturbances, assess historical trends, and allow for effective and actionable kelp forest management. Here, we demonstrate how Kelpwatch can be used to analyze long-term trends in kelp canopy across regions, quantify spatial variability in the response to and recovery from the 2014 to 2016 marine heatwave events, and provide a local analysis of kelp canopy status around the Monterey Peninsula, California. We found that 18.6% of regional sites displayed a significant trend in kelp canopy area over the past 38 years and that there was a strong latitudinal response to heatwave events for each kelp species. The recovery from heatwave events was more variable across space, with some local areas like Bahía Tortugas in Baja California Sur displaying high resilience while kelp canopies around the Monterey Peninsula continued a slow decline and patchy recovery compared to the rest of the Central California region. Kelpwatch provides near real time spatial data and analysis support and makes complex earth observation data actionable for scientists and managers, which can help identify areas for research, monitoring, and management efforts.

Introduction

Along the west coast of North America, underwater forests of kelp provide the foundation for a productive and diverse nearshore ecosystem [1]. The dominant and iconic species of kelp in this region are giant kelp (*Macrocystis pyrifera*) and bull kelp (*Nereocystis luetkeana*), both of

which create large, floating canopies. Both species have high rates of primary production [2] and create complex structure [3], thereby providing food and habitat for many ecologically and economically important species. However, the abundance of these kelp species fluctuates rapidly and is sensitive to environmental changes [4]. Stressors such as climate change, overgrazing, and coastal development have been linked to declines in kelp abundance [5] and there is high spatial variability in the response of kelp forests to changing environmental conditions [6].

From 2014 to 2016 the west coast of North America experienced a series of extreme marine heatwaves that had significant impacts to coastal marine ecosystems [7,8] and was the warmest three-year period on record for the California Current [9]. This heatwave period initially led to widespread declines in the abundance of giant and bull kelp [10,11], but the magnitude and duration of these impacts varied widely. In northern California, the combined effects of the heatwaves, the loss of an important sea urchin predator (sunflower sea stars) due to disease [12], and a subsequent explosion in sea urchin populations led to a collapse in bull kelp abundance, with devastating ecological and economic impacts [11,13]. However, despite the regional loss of sunflower sea stars [12], bull kelp populations in southern Oregon were relatively insensitive to the heatwave events [14]. Around the Monterey Peninsula in Central California, increased sea urchin abundance has reduced the once expansive giant kelp forests to a patchwork of urchin barrens and kelp stands that are maintained by sea otters (an important sea urchin predator) selectively feeding on healthy urchins within the remaining kelp areas [15]. In southern California and across the Baja California Peninsula there were widespread declines in giant kelp abundance immediately following the heatwave events, but recovery in subsequent years was spatially variable [10].

Frequent and widespread monitoring of kelp forests is crucial for understanding patterns and drivers of kelp forest trends and their response to disturbances, which is a key component of effective kelp forest ecosystem-based management [16]. Many species of kelp (including bull kelp and giant kelp) have populations that are highly variable through time [17,18]. Boom and bust

cycles are common, and collapse of kelp forests can be sudden [13,19]. Kelp forest dynamics are also highly variable on small spatial scales (e.g., kms, [20]), which leads to high amounts of variability in patterns of resilience, even following widespread disturbance events such as continental scale marine heatwaves [10,21].

Remote sensing is a powerful tool for monitoring canopy-forming kelps such as bull kelp and giant kelp, and recent increases in the availability of airborne and spaceborne imagery is enabling regular monitoring across multiple space and time scales [5,14,22]. For example, inexpensive small unoccupied aerial systems (UAS) can provide very high-resolution monitoring of canopy extent at local scales [23,24], constellations of CubeSats can provide high resolution data on regional scales [25], while moderate resolution satellites can be used to map kelp at global scales [26,27]. The Landsat satellite program is particularly valuable for kelp monitoring, as it provides imagery with continuous global coverage at a 30 m resolution since 1984. This dataset can be used to detect long-term trends in kelp abundance and put recent changes in a broader historical context [18].

Landsat imagery has been used to map both giant kelp and bull kelp extent on seasonal time scales from 1984 to present for the west coast of the United States and Baja California, Mexico [14,18,28–30] and other regions of the world [27,31,32]. One of the most valuable aspects of this dataset is its extensive spatial and temporal coverage, especially for distinguishing the impacts of climate change on kelp populations from other sources of variability [5]. However, the size of the dataset also makes it difficult to use, especially for those without extensive experience working with large geospatial datasets and more complicated file formats. This accessibility barrier has limited the use of the Landsat dataset for mapping and monitoring canopy-forming kelps.

To increase accessibility of Landsat imagery among researchers, management agencies, and the public, we created Kelpwatch.org, a visualization and analysis web tool that allows users to select a region, time frame, and season(s) of interest to interactively display changes in kelp

canopy over time and freely download data. The primary objective of Kelpwatch.org is to make published kelp canopy data from Landsat imagery actionable for restoration practitioners and researchers, and promote data-driven resource management (e.g., targeted restoration efforts, adaptively managing kelp harvest leases, changing fisheries seasons or catch limits). Analogous web tools have demonstrated success in facilitating data-driven management of other foundational ecosystems by making earth observation data actionable (e.g., Global Forest Watch, Allen Coral Atlas, Global Mangrove Watch; [33–36]).

Kelpwatch.org (hereafter referred to as Kelpwatch) provides a user-friendly interface to analyze and download seasonal kelp canopy observations at 30 m resolution for the west coast of North America from central Baja California, Mexico to the Washington-Oregon border since 1984. To demonstrate the types of analyses that can be completed using Kelpwatch, we used data downloaded directly from Kelpwatch to ask the following questions: (1) What were the regional trends in kelp canopy abundance over the past 38 years? (2) What were the spatial patterns in the resistance and resilience of kelp canopy to the 2014 to 2016 marine heatwave events? and (3) How do local scale patterns in recent kelp canopy area around the Monterey Peninsula, California compare to historical data?

Methods

Kelpwatch Platform

We developed Kelpwatch to make the Landsat kelp canopy dataset actionable via a user-friendly web tool that allows users to visualize changes in kelp canopy dynamics over time. While the kelp canopy dataset is publicly available [28], the size and file format (netCDF) of the dataset makes it difficult to use for those without data science or coding experience. For example, it does not easily load into commonly used GIS/remote sensing software such as QGIS, ArcGIS, ENVI, or ERDAS IMAGINE. The underlying challenge is the combination of a large geographical extent (Oregon, USA through Baja California Sur, Mexico) and moderate spatial resolution (30 m) that

would result in large data files if every single cell, most of them containing open ocean or land (i.e., no kelp canopy), would be represented. Furthermore, the multi-decade length of the dataset, consisting of seasonal means, standard errors, and number of satellite overpasses, makes time series analysis difficult on GIS platforms.

Kelpwatch consists of three elements: (1) a cloud-based backend microservice that makes the data accessible and queryable through an application programming interface (API), (2) a tiling service that serves the classified kelp pixels as a layer to be consumed and displayed by a web map, and (3) a JavaScript-based frontend user interface providing access to the data in any web browser. The frontend was designed to offer simple, intuitive, and informative exploration of the data (Fig 1). Kelpwatch offers users multiple ways to visualize kelp canopy, including animations of dynamics over time and graphs of changes in canopy coverage within a selected area of interest. Importantly, aggregated kelp data within a given geographic and temporal extent can be downloaded as a comma-separated value (csv) file.

Fig 1. Kelpwatch Web Interface. a.) Visualization of map showing spatial extent of kelp canopy dynamics assessed here. b.) Zoomed in map view of the Monterey Peninsula showing kelp canopy area during the summer of 2004 in shades of blue to green. Unoccupied kelp habitat, or areas where kelp has been observed in the past but is not currently present, is shown in gray and areas obscured by cloud cover for the season (i.e., no data) are shown in white. The blue shaded box shows one of the 10 x 10 km cells used in this study and a quarterly (3-month) time series of kelp area within that cell is shown at the bottom (gray lines represent percent cloud cover of that region through time.

Estimates of Kelp Canopy Area Dynamics using Landsat Imagery

Estimates of kelp canopy area were determined using a time series of Landsat satellite imagery across the coasts of Oregon and California, USA, and Baja California Norte and Baja

California Sur, Mexico. This spatial domain covers regions inhabited by two dominant surface canopy forming kelp species, with bull kelp forming the vast majority of kelp canopies throughout Oregon and northern California, and giant kelp in central and southern California as well as the Baja California Peninsula [1]. Imagery was downloaded as 30 meter resolution Collection 1 Level 2 Surface Reflectance products from the United States Geological Survey (https://earthexplorer.usgs.gov/) across four Landsat sensors (Landsat 4 Thematic Mapper, Landsat 5 Thematic Mapper, Landsat 7 Enhanced Thematic Mapper Plus, and Landsat 8 Operational Land Imager) from 1984 to 2021 (Fig S1; Table S1). Each Landsat sensor acquires an image every 16 days and an image is provided every eight days when two sensors were operational (1999 to 2011 and 2013 to present). Images were selected if at least part of the coastline was not obscured by cloud cover. Clouds were masked using the pixel quality assurance band included with each image. Since kelp canopy is usually restricted to a narrow swath along the coast (< 1 km) we masked land using a combination of a digital elevation model and a derived intertidal mask. The Advanced Spaceborne Thermal Emission and Reflection Radiometer (ASTER) 30 m digital elevation model (https://www.jspacesystems.or.jp/ersdac/GDEM/E/) was used to identify and mask any pixel with an elevation greater than zero meters. A single cloud free image for each Landsat path/row acquired at a negative low tide was used to identify intertidal pixels. The Modified Normalized Difference Water Index (MNDWI; [37]) utilizes the shortwave infrared and green spectral bands to derive an index value for each pixel and can separate land exposed during low tide from seawater without interference from floating subtidal kelp canopies. All pixels with a MNDWI index value of less than 0.1 were included in the intertidal mask. After the image classification and processing step described below, pixels adjacent to land with strong, significant negative relationships between the estimated kelp canopy area and tidal height were flagged and plotted on high resolution satellite imagery in Google Earth to confirm that these pixels were not located in intertidal areas. The pixels were manually removed if they were found to be within the intertidal zone. All tidal height measurements coincided with the time of Landsat

image acquisition and were generated from the closest tide station to the center of the image using the Matlab function t_xtide [38].

Once clouds and land were masked, pixels were classified using the binary decision tree classifier described in [18] from band normalized Landsat imagery. The classifier utilizes six spectral bands (blue, green, red, near infrared, and the two shortwave infrared bands) to classify each pixel into four classes (kelp canopy, seawater, cloud, or land, where the cloud and land classes remove pixels not identified in the masks). Multiple endmember spectral mixture analysis (MESMA; [39]) was then used to estimate the proportion of kelp canopy within each 30 m pixel classified as kelp canopy using the blue, green, red, and near infrared spectral bands (see [18] for detailed methods). Since the MESMA model relies heavily on the near infrared light reflected by kelp canopy floating directly on the ocean surface, we estimated the fractional cover of emergent kelp canopy within each pixel, hereafter referred to as kelp canopy area. Any portion of the kelp thallus submerged more than a few centimeters below the surface is likely not detected. Fractional kelp canopy within each pixel was converted to kelp canopy area by multiplying the fractional value by the area of the Landsat pixel (900 m^2). Canopy area was then provided to Kelpwatch as quarterly (3-month) mean canopy area by calculating the mean kelp canopy area for each pixel for all Landsat images acquired during that quarter [28].

Regional Trends in Kelp Canopy Area

Regional trends in kelp canopy area were assessed by summing all kelp containing pixels within 10 x 10 km cells from the Oregon/Washington border to the southern range limit of canopy forming kelp detected in the time series near Punta Prieta, Baja California Sur, Mexico. The corner coordinates of each cell were encoded into GeoJSON files and uploaded to Kelpwatch. The kelp canopy data was then downloaded from Kelpwatch and cells with less than 500 pixels of potential kelp habitat were excluded from the analysis. This resulted in 97.8% of the total kelp canopy area from the complete time series being included within the 10 x 10 km cells. Regional time series

from six regions (hereafter referred to as Oregon, Northern California, Central California, Southern California, Baja California Norte, and Baja California Sur; Fig S2), were produced as a sum of all cells within each region's domain. If greater than 25% of pixels did not have a cloud-free acquisition during a quarter, the entire 10 x 10 km cell was treated as missing data for that quarter. To account for seasonal differences in peak annual canopy area that may result from differences in species phenology or geography [40], the maximum canopy area was determined for each cell for each year from 1984 to 2021. Annual canopy area was not determined for a particular year if more than half of that region's cells were missing more than one quarter. The trend of annual kelp canopy area through time in each region, as well as each individual 10 x 10 km cell, was assessed using a generalized least squares regression model (R package nlme; [41]) with an auto-regressive model to account for temporal autocorrelation in the model residuals. As the effects of temporal autocorrelation may change due to species or regional environmental conditions, three auto-regressive processes were applied to each model (zero, first, and second order) and the best model was selected by minimizing the Akaike Information Criterion. To account for differences in available kelp habitat between each 10 x 10 km cell and to express the trend as a percentage increase/decrease, the canopy area time series of each cell was normalized by the maximum canopy area observed between 1984 to 2021.

Regional Kelp Resistance and Resilience

Between 2014 to 2016 the west coast of North America experienced a series of extreme marine heatwaves, with temperature anomalies of 2 to 3°C across the entire California Current [42,43]. Regional kelp declines and recovery from this historic heatwave period were assessed by examining the resistance and resilience of kelp canopy within the 10 x 10 km cells. The baseline period was set to the five-year period immediately preceding the heatwave events (2009 to 2013) following [10]. This baseline period was characterized by cool ocean conditions and

represents the most recent period of moderate to high kelp canopy area across the study domain. Resistance, or the degree to which a system has changed during and shortly following a disturbance event [44], was calculated as the minimum annual kelp canopy area from 2014 to 2016 relative to the baseline period. Resilience, or the degree of recovery of initial structure after a disturbance [45], was calculated as the mean annual kelp canopy area from 2017 to 2021 relative to the baseline period. Latitudinal trends in resistance and resilience were examined using Pearson correlations, a constant value of 1% was added, and values were log transformed to meet the assumptions of the model. To put the effects of the unprecedented marine heatwaves into historical perspective [9], mean kelp canopy area since the beginning of the heatwave events (2014 to 2021) was compared to the historical mean canopy area from 1984 to 2013 for each 10 x 10 km cell.

Local Assessment of Kelp Canopy Area around Monterey Peninsula

The area surrounding the Monterey Peninsula exhibited an overall loss in kelp canopy following the 2014 to 2016 marine heatwave events, with five 10 x 10 km cells showing negative long-term trends, low resilience, and low amounts of recent canopy compared to the historical mean. To further investigate these patterns at the local scale (across ~40 km of coastline), kelp canopy area was assessed by summing all kelp containing pixels within 1 x 1 km cells across the affected area. Spatial synchrony of kelp canopy declines dramatically within 200 m [20,46], so the cell size of 1 km was chosen to avoid spatial autocorrelation processes. Similar to the regional analysis, the corner coordinates of the cells were encoded into GeoJSON files, the data were downloaded from Kelpwatch, and cells with less than 25 pixels of potential kelp habitat were excluded from the analysis. If greater than 25% of pixels did not have a cloud-free acquisition during a quarter, the entire 1 x 1 km cell was treated as missing data for that quarter. Annual maximum kelp canopy area was calculated similarly to the regional analysis and a year with two or more missing quarters was treated as missing data. Mean canopy area from 2014 to 2021 was

used to calculate the recent state of the kelp canopy since the marine heatwave events relative to the historical mean from 1984 to 2013.

Results

Regional Trends in Kelp Canopy Dynamics

Kelp canopy area dynamics were assessed for Oregon, Central California, and Southern California regions with either a complete 38-year time series or one missing year (Fig 2). The Northern California and Baja California Norte regions had three and four missing years, respectively (mostly due to the coincidence of cloud cover and a single Landsat sensor early in the time series), while Landsat imagery does not exist for much of Baja California Sur before the mid 1990's resulting in 10 missing years (Table S1). In Oregon, the vast majority of canopy forming kelp was observed in the southern portion of the state south of Cape Blanco (Fig 3a). At these large reefs, there were three periods of high kelp canopy across the time series with two events in the mid-1980's to 1990 and one in the late 1990's, which resulted in a significant regional decline of 0.8% per year across the time series (standard error = 0.2%, $p = 0.007$). The Northern California region displayed multiple periods of high kelp canopy across the time series with peaks in 1999, 2008, and 2012 followed by a prolonged period of low canopy after the 2014 to 2016 marine heatwave events. Due to the high variability in kelp canopy area throughout the time series, there was no significant long-term trend (-0.7% per year, SE = 0.4%, $p = 0.123$). Central California showed high kelp canopy in the late 1980s and early 1990s with low canopy area during the 1997/98 El Niño event and from 2019 to 2021. This combination of high kelp canopy area early in the time series and recent losses resulted in a significant regional decline of 0.6% per year (SE = 0.3%, $p = 0.044$). Southern California also showed high kelp canopy in the late 1980s and early 1990s and a prolonged low canopy period in the late 1990s. This period was accompanied by a rapid recovery following the 1997/98 El Niño event with peak canopy area from

2003 to 2005. Despite a gradual decline in canopy area since the 2005 peak, there was no significant regional change detected in Southern California (-0.2% per year, SE = 0.5%, p = 0.711). Baja California Norte also displayed low kelp canopy in the late 1990s followed by a steep increase culminating in peak canopy area in 2009. Kelp canopy area has been variable since the peak and no significant regional trend was detected (0.1% per year, SE = 0.4%, p = 0.835). Data for Baja California Sur was missing for the early part of the time series, however there were two distinct kelp canopy peaks in 2000 and 2014. There was a steep decline in kelp canopy area following the 2014 to 2016 marine heatwave events and a strong recovery in 2018. There was no significant regional trend detected (0.4% per year, SE = 0.5%, p = 0.381).

Fig 2. Regional Time Series. Annual time series of kelp canopy area from each of the six study regions.

Fig 3. Significant Trends in Kelp Canopy. Map of 10 x 10 km cells with significant long-term annual trends across the time series. Annual time series of example cells are shown on the left.

When examining the 10 x 10 km cells across the entire study domain, 18.6% of the cells displayed a significant trend ($p < 0.05$; 32 of 172 cells), with 14.5% of the cells showing a negative trend (25 cells) and 4.0% showing a positive trend (7 cells; Table 1). Oregon was the only region that contained a majority of cells with significant trends. The only regions where greater than 10% of cells showed negative long-term trends other than Oregon (55.6%) were Northern California (20.0%) and Central California (35.5%), while Southern California (8.6%) and Baja California Norte (2.9%) had less than 10% of cells with negative trends. Baja California Sur showed no cells with negative long-term trends across the time series. Positive trends were only observed in cells within Central and Southern California and Baja California Norte and Baja California Sur. Within Central California, cells with negative trends were clustered around and to the south of the

Monterey Peninsula while all cells with negative trends in Southern California were found at sites along the offshore Channel Islands (Fig 3c).

Table 1. Regional Trends in Kelp Canopy.

Region	Total Cells	Positive Trend	Negative Trend	No Significant Trend
Oregon	9	0 (0%)	5 (55.6%)	4 (44.4%)
Northern CA	15	0 (0%)	3 (20.0%)	12 (80.0%)
Central CA	31	2 (6.5%)	11(35.5%)	18 (58.0%)
Southern CA	58	1 (1.7%)	5 (8.6%)	52 (89.7%)
Baja Norte	35	2 (5.7%)	1 (2.9%)	32 (91.4%)
Baja Sur	24	2 (8.3%)	0 (0%)	22 (91.7%)

Total number of 10 x 10 km cells and the number (percent) of cells with positive, negative, no significant long-term annual trends for each region.

Resistance and Resilience to the 2014 to 2016 Marine Heatwave Events

Resistance to the 2014 to 2016 marine heatwave events varied among regions, with a mean resistance of 20.2% (standard deviation 30.6%) across all 10 x 10 km cells (Fig 4). For areas with predominantly bull kelp canopies, Oregon showed a higher resistance of 40.9% (56.1%) compared to the 2.0% (3.4%) of Northern California canopies remaining during the marine heatwave events compared to the baseline period. For areas with predominantly giant kelp canopies, Central California showed a mean resistance of 52.6% (43.2%), and Southern California and Baja California Norte fared similarly with 15.5% (18.6%) and 14.5% (14.5%), respectively. Kelp canopies in Baja California Sur showed low resistance to the heatwave events with only 1.8% (4.0%) remaining. Resistance to the marine heatwave events was significantly

related to latitude for both giant kelp and bull kelp dominated regions. There was increased log resistance with latitude from Baja California Sur to Central California (giant kelp dominated; $r = 0.606$, $p < 0.001$) and from Northern California to Oregon (bull kelp dominated; $r = 0.761$, $p < 0.001$) although there was considerable local scale variability among the 10 x 10 km cells (Fig 5a; for untransformed data see Fig S3a).

Fig 4. Resistance and Resilience to Marine Heat Wave Events. Maps of kelp canopy resistance (degree to which the canopy changed during the 2014 – 2016 marine heatwave versus the baseline period) and resilience (degree to which the canopy recovered after the marine heatwave versus the baseline period) within the 10 x 10 km cells for the study domain. The letters correspond to the locations shown in Fig 6. The black box corresponds to the area shown in Fig 7.

Fig 5. Latitudinal Trends in Resistance and Resilience. Scatter plots of the a.) resistance and b.) resilience of kelp canopy to the 2014 – 2016 marine heatwave events compared to the baseline period of 2009 to 2013. Areas dominated by giant kelp canopy are shown in blue and areas dominated by bull kelp canopy are shown in red. Note that the y-axes are on a log scale.

Resilience to the marine heatwave events was more variable within each region for areas dominated by giant kelp leading to a weaker significant relationship between log resilience and latitude ($r = 0.304$, $p < 0.001$; Fig 5b; for untransformed data see Fig S3b). However, the relationship was similar for bull kelp dominated areas ($r = 0.747$, $p < 0.001$). While resilience in Northern California remained low after the marine heatwave events with only a 5.7% (standard deviation 6.2%) recovery compared to the baseline period, kelp canopies in Oregon were highly variable, with a mean regional resilience of 253.2% (474.8%). These ranged from less than 10% recovery at Orford Reef to greater than 1400% recovery at Rogue Reef (Fig 6a). In the giant kelp

dominated regions, recovery was strong along most of the Central California coast with a mean regional resilience of 89.6% (61.0%), apart from kelp canopies around and to the south of the Monterey Peninsula. Resilience in Southern California was variable with a mean regional resilience of 70.1% (72.5%) with areas of low resilience occurring in the western half of the Northern Channel Islands and the southern portion of the region. Similarly, resilience in Baja California Norte was also variable with a mean regional resilience of 53.6% (52.6%). The Baja California Sur region showed a mean regional resilience of 72.2% (106.4%; Fig 6b) with strong local variability, for example areas around Punta Eugenia showed high resilience while areas to the immediate north and south displayed little recovery. Overall, 44.4% of the 10 x 10 km cells in Oregon recovered to baseline levels while 0% of Northern California cells fully recovered. Central California and Southern California had a similar proportion of cells recover fully compared to the baseline period, 29.0% and 25.9% respectively. Baja California Norte showed the lowest percentage of cells achieving full recovery in the range of giant kelp dominance with 17.1% and Baja California Sur had 29.2% of cells fully recover from the marine heatwave events.

Fig 6. False Color Landsat Images Showing Change in Kelp Canopy. a.) Rogue Reef, Oregon, b.) Bahía Tortugas, Baja California Sur, and c.) Monterey Peninsula and Carmel Bay, California before, during, and after the marine heatwave events. Locations shown in Fig 4. Kelp canopy has high reflectance in the near-infrared which has been colored red in these images for visualization purposes. The numbers in bottom left image represent 1. Pescadero Point, 2. Carmel Point, and 3. Point Lobos.

Local Patterns of Kelp Canopy Around Monterey Peninsula

The cluster of five 10 x 10 km cells surrounding and to the south of the Monterey Peninsula showed some of the strongest declines across the time series (Fig 3; Fig 6c), low resilience despite relatively high resilience across most of the Central California region (Fig 4, Fig S2), and

low overall kelp canopy during and after the heatwave events compared to the historical mean (Fig S4). The seasonal time series of kelp canopy area for the Monterey Peninsula displayed steep declines during the 2014 to 2016 marine heatwave events and continued to decline post-heatwave (Fig 7a). The period of decline (2014 to 2021) represents the longest consecutive period of low canopy kelp cover around and to the south of the Monterey Peninsula in the entire time series, with canopy area during this period representing 17.4% of the mean canopy area from 1984 to 2013. When examined at the local scale (1 x 1 km cells), 91.1% of cells showed less than 50% of their historical pre-heatwave average (1984 to 2013) during the period from 2014 to 2021 (Fig 7b). Furthermore, 46.7% of the cells were less than 10% of their historical pre-heatwave average, while only 6.7% of cells were at or above their historical pre-heatwave average.

Fig 7. Kelp Dynamics around the Monterey Peninsula. a.) Seasonal time series of kelp canopy area for the Monterey Peninsula. b.) Mean annual canopy area from 2014 to 2021 in 1 x 1 km cells as a percentage of mean annual canopy area from 1984 to 2013. Values of 100% represent kelp canopy areas greater than or equal to the historical mean.

Discussion

Long-term Trends in Kelp Canopy Across Regions

Significant long-term trends in kelp forest canopy area were observed at the 10 x 10 km scale and across entire regions. Kelp canopy in Oregon was characterized by three short periods of high canopy area early and in the middle of the time series, followed by a longer period of moderate kelp canopy starting the mid-2000's, resulting in a significant, overall regional decline from 1984 to 2021 (Fig 2). Total kelp canopy area in Oregon was dominated by the dynamics on Orford, Blanco, and MacKenzie reefs (Fig 3a), a large rocky reef complex southwest of Cape Blanco totaling ~50 km^2 with depths ranging from 10 to 25 m [47]. Five of the nine 10 x 10 km

cells in the Oregon region declined over the study period, the only region where a majority of cells showed significant long-term trends (Table 1). While there are a paucity of studies examining subtidal kelp dynamics and environmental drivers in Oregon, [14] used Landsat imagery to assess five of the region's largest kelp forests from 1984 to 2018. Two of the five forests examined displayed long-term declines, including Orford Reef [14]. Kelp forests in Oregon have also been periodically assessed via aerial imagery by the Oregon Department of Fish and Wildlife with imagery collected in 1990, 1996 to 1999, and 2010 [47–51]. A change in the method of image collection from color-infrared photography (1990's) to digital multispectral imagery (2010) made intercomparison difficult as photographs from the 1990's were delineated by hand while individual 1-meter pixels were classified as kelp canopy from the multispectral imagery [51]. Without robust calibration between sensors through time, as done with the Landsat sensors [18], long-term trend analysis is impossible.

Kelp forests off the coast of Northern California have experienced historic lows from 2014 to 2021 [11,13,24], however, while 20% of the 10 x 10 km cells showed a negative trend, a significant regional decline was not observed in the full time series. Kelp canopy was highly dynamic across the region, with three periods of high multiyear kelp area during the late 1980's to early 1990's, late 1990's to early 2000's, and late 2000's to early 2010's, with the two highest years occurring in 2008 and 2012 (Fig 2). Despite the recent period of low or absent kelp canopy across the region from 2014 to 2021, the interannual oscillatory nature of the canopy throughout the time series and the historic high levels of canopy present in the years immediately preceding the marine heatwave (2008, 2012 to 2013) likely contributed to the lack of a negative trend. Even with the limited recovery observed in 2021 (Fig 2), a continuation of current low kelp canopy conditions for the next two to three years would likely result in a significant long-term regional

decline. The Central California region did display a significant regional decline in canopy area across the time series (Fig 2), driven by a large decrease in canopy area around the Monterey Peninsula since 2014 (Fig 3b; see *Local Declines Around Monterey Peninsula*). High kelp canopy area early in the time series resulting from both high canopy density and large canopy extent likely contributed to this negative trend. The Central California region represents a transition zone between the two major canopy forming kelp species but is mostly dominated by giant kelp (*Macrocystis pyrifera*; [1]). While over 35% of 10 x 10 km cells displayed negative trends (Table 1), Central California also possessed two cells with positive trends, including the northernmost cell near Point Año Nuevo, which showed increasing post-heatwave canopy area.

Southern California and Baja California Norte both showed a low percentage of cells with significant trends (~10%), with every Southern California cell with significant trends located on the offshore Channel Islands (Fig 3c). Both regions suffered major reductions in plant and stipe density and canopy area during the 1997/1998 El Niño event, reaching regional minimums in 1998 (Fig 2; [52,53]). However, both regions responded positively to the 1999/2000 La Niña event and canopy area continued to increase regionally with positive North Pacific Gyre Oscillation index values and the associated elevated seawater nutrients [6,54] with regional maximums in 2005 for Southern California and 2009 for Baja California Norte (Fig 2). Baja California Sur had the shortest regional time series due to a lack of available imagery at the beginning of the time series (Table S1). While no regional trend was detected, the two positive long-term trends from individual 10 x 10 km cells should be treated with skepticism since missing data occurred during a period when canopy area was relatively high across regions.

The relationship between regional kelp dynamics and decadal marine climate oscillations [6,55,56] produce multiyear periods of high (or low) kelp canopy that make the identification of long-term trends difficult [18]. Additionally, a recent analysis has shown that the synchrony of giant kelp canopy is highly coherent with the North Pacific Gyre Oscillation on long time scales (4 to 10 years; [57]), meaning that sites within regions tend to increase and decrease similarly

according to the fluctuations of the large-scale ocean climate. Since regular oscillatory patterns make the detection of long-term trends difficult [18,58], perhaps the most beneficial use for these data is to investigate the spatial heterogeneity of the response in kelp canopy to major climate events, such as the 2014 to 2016 marine heatwaves. Here, this type of analysis uncovered sub-regional (and potentially local scale) variability in kelp canopy and could allow researchers to hone in on areas showing disparate patterns and elucidate underlying drivers.

Resistance and Resilience to the 2014 - 2016 Marine Heatwave Events

During the summer of 2014, an unprecedented warm water temperature event spread across the Northeastern Pacific leading to negative impacts across both nearshore and pelagic ecosystems [42,59,60]. This marine heatwave, known as 'The Blob', was closely followed by a strong El Niño event in 2015-2016, contributing to an extended period of anonymously high warm ocean temperatures, low seawater nutrients, and low productivity throughout the region [61]. Notably, there were historic and widespread declines in kelp forest ecosystems associated with these events, both in Northern California [13] and Baja California [62], although ecosystem response was not constant across regions [63]. We found that resistance of kelp canopies to the marine heatwave period was low across regions, but positively related to latitude. Cavanaugh and others [10] found that the resistance of giant kelp canopy across Southern and Baja California was associated with an absolute temperature threshold (23°C) and not a relative temperature anomaly. Since ocean temperature generally decreases in the California Current with increasing latitude [64], it is perhaps not surprising that the resistance of kelp canopy to the marine heatwave events was higher in northern regions given that kelp responds strongly to temperatures over an absolute threshold. Interestingly, regions that are primarily composed of bull kelp also exhibited a similar latitudinal response separate from the one displayed by regions dominated by giant kelp (Fig 5a). This implies that each species may possess specific temperature thresholds for growth

and mortality and in fact, recent laboratory experiments show that bull kelp blades maximize elongation rate at 11.9°C with precipitous declines at temperatures above 16°C [65].

While previous marine heatwave events have resulted in short-term declines in kelp abundance across regions, the resilience, or degree of kelp canopy recovery following the heatwave, can be spatially variable and often occur at smaller spatial scales (meters to kilometers; [52]). While a significant positive relationship between resilience and latitude was found for giant kelp, the relationship was more variable when compared to resistance, with examples of high resilience in all four giant kelp dominated regions (Fig 5b). This is a similar result to previous studies that found no clear relationship between large scale temperature and heatwave variables to kelp recovery [10]. One striking example of resilience is the kelp forest that surrounds Bahía Tortugas in Baja California Sur near the southern range limit for giant kelp in the Northern Hemisphere (Fig 6b). This forest displayed high kelp canopy area before the heatwave, a complete loss of canopy during the heatwave, and a complete recovery to greater canopy area in the years following. However, this kelp forest is surrounded by 10 x 10 km cells that displayed little resilience during the five years post-heatwave events (Fig 4), implying a driver acting over a smaller spatial scale than patterns in latitudinal temperature. The coast of Baja California has a varied geometry leading to distinct sub-regional upwelling zones that are oriented parallel to the dominant wind direction [66]. The three upwelling zones located within our Baja California study domain exist at 31.5°N, 29°N, and 27°N and all correspond to cells with high resilience. The sub-regional nature of coastal upwelling, delivering cool, nutrient-rich seawater to the nearshore, may be vital to kelp forest recovery after heatwave events and future studies comparing kelp dynamics to localized upwelling are needed. Regions dominated by bull kelp showed a significant relationship between resilience and latitude, driven by little resilience in Northern California and varied resilience in Oregon. While signs of kelp canopy recovery in Northern California did not begin until 2021, some sites in Oregon displayed increases in canopy area throughout and after the heatwave events. An example of this is Rogue Reef, where little canopy was present prior to

the heatwave, small increases occurred during the heatwave, and a large canopy formed post-heatwave (Fig 6a). This incredible level of resilience (~1400%) is partly driven by lack of canopy during the baseline period, but it represents one of the few areas with increasing kelp canopy during the marine heatwave events. As there are fewer subtidal monitoring programs in Oregon compared to California [67], more work is needed to understand the spatial drivers of kelp forest dynamics across Oregon.

Local Declines Around Monterey Peninsula

While the Central California region exhibited relatively high levels of resilience to the marine heatwave events, the five 10 x 10 km cells surrounding the Monterey Peninsula showed < 30% resilience compared to the baseline period. Prior to the heatwave events, kelp canopy area around the Monterey Peninsula was seasonally dynamic but persistently high on annual time scales, with decreases during the heatwave events of 2014 to 2016 and with further reductions post-2016 (Fig 7a). This cluster of sustained, low resilience cells warranted a local scale analysis made possible by altering the domain of the spatial input polygons uploaded to Kelpwatch. During the post-heatwave years (2014 to 2021) the vast majority of 1 x 1 km cells showed less than 50% of their mean historical canopy area (1984 to 2013) with only a few local scale examples of high resilience (Fig 7b). An examination of the Landsat imagery used to generate the kelp canopy data for Kelpwatch further illustrates these declines. The kelp forests near Pescadero Point (Fig 6c, 1), Carmel Point (Fig 6c, 2), and Point Lobos (Fig 6c, 3) can be clearly seen as the offshore red patches in the false color imagery during September 2011. By September 2016, the Pescadero Point kelp forest canopy (1) had nearly disappeared, Carmel Point (2) was similar in area to 2011 and Point Lobos (3) had been reduced to a few patches. By September 2021, the Pescadero Point kelp forest (1) was showing some patchy recovery, Carmel Point (2) had been reduced to patches and Point Lobos (3) had nearly disappeared. These spatial patterns exposed by Kelpwatch support a recent field-based analysis examining the role of sea otters, an important

predator of herbivorous sea urchins. Smith and others [15] found that the spatial pattern of sea otter foraging was associated with the distribution of energetically profitable urchins, that is, restricted to areas that maintained high kelp densities and well-fed sea urchins. This resulted in a patchy mosaic of kelp forest stands interspersed with sea urchin barrens, possibly enhancing the resistance of existing stands but not directly contributing to the resilience of areas without kelp. While this explains the spatial patchiness and lack of recovery of kelp canopy around the Monterey Peninsula, it does not explain why this subregion was less resilient than other areas in Central California. The sustained decline in kelp canopy around the Monterey Peninsula detected using the Kelpwatch tool represents the longest period of low canopy cover for this area over the length of the Landsat time series, suggesting that more research and monitoring attention should be directed at this location. Understanding differences in environmental conditions and trophic interactions around the Monterey Peninsula and nearby locations that have exhibited high kelp canopy resilience may shed light on important drivers that are best assessed by instrumented moorings and diver-based survey methods. This case study demonstrates how a decision-support tool like Kelpwatch can be used to make complex data actionable for managers, restoration practitioners, and researchers, and promote data-driven resource management.

Conclusions

Over the past decade, there has been an increased focus on the long-term declines of kelp forests both regionally and globally, usually in the context of warming ocean conditions, competition with other reef space holders, and increases in herbivore abundance [68–71]. While kelp forests in many regions have undoubtedly experienced severe and unprecedented declines in recent years [11,72], time series of kelp dynamics are often limited by short durations or punctuated field campaigns. These time series limitations can obscure the true nature of kelp forest change especially given the rapid dynamics of kelp. For example, a recently observed decline may be related to a decadal marine climate oscillation and similar periods of low kelp

abundance may have occurred before the time series was initiated or were missed due to logistical or funding constraints. Therefore, it is essential to produce a long, continuous, and calibrated time series in order to put recent declines in the context of long-term dynamics. While Landsat observations can be limited by cloud cover and can only detect fluctuations in surface canopy, the uninterrupted satellite continuity (1984 to present), rapid repeat frequency (16 days from 1984 to 1998; 8 days from 1999 to present), and large spatial domain (global) offer an unparalleled opportunity to track kelp forest dynamics [18,73]. The assessment of continuous kelp dynamics allows for the observation of decadal cycles in canopy cover that often result from changes in regional nutrient regimes (e.g., the North Pacific Gyre Oscillation; [6,54,56]) or sudden regional scale crashes and recoveries in canopy cover resulting from El Niño and La Niña events, respectively [21]. Recently, an ensemble of climate models was used to determine the appropriate time series length needed to distinguish a climate change precipitated trend from natural variability for several biogeochemically relevant marine variables and found that time series of at least 40 years in length are necessary to define the natural variability of biotic variables (phytoplankton chlorophyll concentration and production dynamics; [58]). With close to 40 years of observations as of the time of this analysis, the Landsat-derived data available on Kelpwatch are beginning to approach the length necessary to observe changes in kelp canopy across decadal cycles and detect long-term trends.

Tools like Kelpwatch make earth observation data actionable and will help scientists and managers identify areas to focus research and monitoring efforts to understand how kelp forests respond to marine heatwaves and other pressures, and to place these dynamics in historical context to inform strategic management interventions. All the analyses in this study were completed using data downloaded directly from the platform and analyzed in commonly used geospatial or statistical programs for transparency and reproducibility. Having a calibrated, open-access, and continuous time series of kelp abundance data puts the ability to examine near real-

time trends in kelp abundance and spot problem areas for kelp loss in the hands of scientists and managers.

Acknowledgements

We thank Steve Lonhart, Kristen Elsmore, and Dana Morton for reviews of the manuscript.

References

1. Carr MH, Reed DC. Shallow Rocky Reefs and Kelp Forests. Shallow Rocky Reefs and Kelp Forests. University of California Press; 2016. pp. 311–336. doi:10.1525/9780520962170-021

2. Mann, K.H. Ecology of coastal waters. Malden, Massachusetts, USA: Blackwell; 2000.

3. Miller RJ, Lafferty KD, Lamy T, Kui L, Rassweiler A, Reed DC. Giant kelp, Macrocystis pyrifera, increases faunal diversity through physical engineering. Proc R Soc B Biol Sci. 2018;285: 20172571. doi:10.1098/rspb.2017.2571

4. Schiel DR, Foster MS. The Biology and Ecology of Giant Kelp Forests. University of California Press; 2015.

5. Cavanaugh KC, Bell T, Costa M, Eddy NE, Gendall L, Gleason MG, et al. A Review of the Opportunities and Challenges for Using Remote Sensing for Management of Surface-Canopy Forming Kelps. Front Mar Sci. 2021;8: 1536. doi:10.3389/fmars.2021.753531

6. Bell TW, Cavanaugh KC, Reed DC, Siegel DA. Geographical variability in the controls of giant kelp biomass dynamics. J Biogeogr. 2015;42: 2010–2021. doi:https://doi.org/10.1111/jbi.12550

7. Brodeur RD, Auth TD, Phillips AJ. Major Shifts in Pelagic Micronekton and Macrozooplankton Community Structure in an Upwelling Ecosystem Related to an Unprecedented Marine Heatwave. Front Mar Sci. 2019;6. Available: https://www.frontiersin.org/article/10.3389/fmars.2019.00212

8. Piatt JF, Parrish JK, Renner HM, Schoen SK, Jones TT, Arimitsu ML, et al. Extreme mortality and reproductive failure of common murres resulting from the northeast Pacific marine heatwave of 2014-2016. PLOS ONE. 2020;15: e0226087. doi:10.1371/journal.pone.0226087

9. Thompson AR, Ben-Aderet NJ, Bowlin NM, Kacev D, Swalethorp R, Watson W. Putting the Pacific marine heatwave into perspective: The response of larval fish off southern California to unprecedented warming in 2014–2016 relative to the previous 65 years. Glob Change Biol. 2022;28: 1766–1785. doi:10.1111/gcb.16010

10. Cavanaugh KC, Reed DC, Bell TW, Castorani MCN, Beas-Luna R. Spatial Variability in the Resistance and Resilience of Giant Kelp in Southern and Baja California to a Multiyear Heatwave. Front Mar Sci. 2019;6. doi:10.3389/fmars.2019.00413

11. McPherson ML, Finger DJI, Houskeeper HF, Bell TW, Carr MH, Rogers-Bennett L, et al. Large-scale shift in the structure of a kelp forest ecosystem co-occurs with an epizootic and marine heatwave. Commun Biol. 2021;4: 1–9. doi:10.1038/s42003-021-01827-6

12. Harvell CD, Montecino-Latorre D, Caldwell JM, Burt JM, Bosley K, Keller A, et al. Disease epidemic and a marine heat wave are associated with the continental-scale collapse of a pivotal predator (Pycnopodia helianthoides). Sci Adv. 2019;5: eaau7042. doi:10.1126/sciadv.aau7042

13. Rogers-Bennett L, Catton CA. Marine heat wave and multiple stressors tip bull kelp forest to sea urchin barrens. Sci Rep. 2019;9: 15050. doi:10.1038/s41598-019-51114-y

14. Hamilton SL, Bell TW, Watson JR, Grorud-Colvert KA, Menge BA. Remote sensing: generation of long-term kelp bed data sets for evaluation of impacts of climatic variation. Ecology. 2020;101: e03031. doi:https://doi.org/10.1002/ecy.3031

15. Smith JG, Tomoleoni J, Staedler M, Lyon S, Fujii J, Tinker MT. Behavioral responses across a mosaic of ecosystem states restructure a sea otter–urchin trophic cascade. Proc Natl Acad Sci. 2021;118. doi:10.1073/pnas.2012493118

16. Hamilton SL, Gleason MG, Godoy N, Eddy N, Grorud-Colvert K. Ecosystem-based management for kelp forest ecosystems. Mar Policy. 2022;136: 104919. doi:10.1016/j.marpol.2021.104919

17. Tegner M, Dayton P, Edwards P, Riser K. Large-scale, low-frequency oceanographic effects on kelp forest succession: a tale of two cohorts. Mar Ecol Prog Ser. 1997;146: 117–134. doi:10.3354/meps146117

18. Bell TW, Allen JG, Cavanaugh KC, Siegel DA. Three decades of variability in California's giant kelp forests from the Landsat satellites. Remote Sens Environ. 2020;238: 110811. doi:10.1016/j.rse.2018.06.039

19. Wernberg T, Smale DA, Tuya F, Thomsen MS, Langlois TJ, De Bettignies T, et al. An extreme climatic event alters marine ecosystem structure in a global biodiversity hotspot. Nat Clim Change. 2013;3: 78–82.

20. Cavanaugh KC, Kendall BE, Siegel DA, Reed DC, Alberto F, Assis J. Synchrony in dynamics of giant kelp forests is driven by both local recruitment and regional environmental controls. Ecology. 2013;94: 499–509. doi:10.1890/12-0268.1

21. Edwards M, Estes J. Catastrophe, recovery and range limitation in NE Pacific kelp forests: a large-scale perspective. Mar Ecol Prog Ser. 2006;320: 79–87. doi:10.3354/meps320079

22. Schroeder SB, Dupont C, Boyer L, Juanes F, Costa M. Passive remote sensing technology for mapping bull kelp (Nereocystis luetkeana): A review of techniques and regional case study. Glob Ecol Conserv. 2019;19: e00683. doi:10.1016/j.gecco.2019.e00683

23. Cavanaugh KC, Cavanaugh KC, Bell TW, Hockridge EG. An Automated Method for Mapping Giant Kelp Canopy Dynamics from UAV. Front Environ Sci. 2021;8: 301. doi:10.3389/fenvs.2020.587354

24. Saccomanno VR, Bell TW, Pawlak C, Stanley C, Cavanaugh KC, Hohman R, et al. Using Unoccupied Aerial Vehicles (UAVs) to map and monitor changes in emergent kelp canopy after an ecological regime shift. in review.

25. Cavanaugh KC, Cavanaugh KC, Pawlak C, Bell TW, Saccomanno VR. CubeSats show persistence of bull kelp refugia amidst a regional collapse in California. in review.

26. Mora-Soto A, Palacios M, Macaya EC, Gómez I, Huovinen P, Pérez-Matus A, et al. A High-Resolution Global Map of Giant Kelp (Macrocystis pyrifera) Forests and Intertidal

Green Algae (Ulvophyceae) with Sentinel-2 Imagery. Remote Sens. 2020;12: 694. doi:10.3390/rs12040694

27. Houskeeper HF, Rosenthal IS, Cavanaugh KC, Pawlak C, Trouille L, Byrnes JEK, et al. Automated satellite remote sensing of giant kelp at the Falkland Islands (Islas Malvinas). PLOS ONE. 2022;17: e0257933. doi:10.1371/journal.pone.0257933

28. Bell TW, Cavanaugh KC, Siegel DA. SBC LTER: Time series of quarterly NetCDF files of kelp biomass in the canopy from Landsat 5, 7 and 8, since 1984 (ongoing). Environ Data Initiat. 2022;ver 16. doi:https://doi.org/10.6073/pasta/93b47266b20bc1782c8df9c36169e372

29. Finger DJI, McPherson ML, Houskeeper HF, Kudela RM. Mapping bull kelp canopy in northern California using Landsat to enable long-term monitoring. Remote Sens Environ. 2021;254: 112243. doi:10.1016/j.rse.2020.112243

30. Arafeh-Dalmau N, Cavanaugh KC, Possingham HP, Munguia-Vega A, Montaño-Moctezuma G, Bell TW, et al. Southward decrease in the protection of persistent giant kelp forests in the northeast Pacific. Commun Earth Environ. 2021;2: 1–7. doi:10.1038/s43247-021-00177-9

31. Friedlander AM, Ballesteros E, Bell TW, Giddens J, Henning B, Hüne M, et al. Marine biodiversity at the end of the world: Cape Horn and Diego Ramírez islands. PLOS ONE. 2018;13: e0189930. doi:10.1371/journal.pone.0189930

32. Friedlander AM, Ballesteros E, Bell TW, Caselle JE, Campagna C, Goodell W, et al. Kelp forests at the end of the earth: 45 years later. Chapman M (Gee) G, editor. PLOS ONE. 2020;15: e0229259. doi:10.1371/journal.pone.0229259

33. Asner GP, Vaughn NR, Heckler J, Knapp DE, Balzotti C, Shafron E, et al. Large-scale mapping of live corals to guide reef conservation. Proc Natl Acad Sci. 2020;117: 33711–33718. doi:10.1073/pnas.2017628117

34. Kennedy E, Roelfsema C, Lyons M, Kovacs E, Borrego-Acevedo R, Roe M, et al. Reef Cover: a coral reef classification to guide global habitat mapping from remote sensing. bioRxiv; 2020. p. 2020.09.10.292243. doi:10.1101/2020.09.10.292243

35. Zhang D, Wang H, Wang X, Lü Z. Accuracy assessment of the global forest watch tree cover 2000 in China. Int J Appl Earth Obs Geoinformation. 2020;87: 102033. doi:10.1016/j.jag.2019.102033

36. Bunting P, Rosenqvist A, Hilarides L, Lucas RM, Thomas N. Global Mangrove Watch: Updated 2010 Mangrove Forest Extent (v2.5). Remote Sens. 2022;14: 1034. doi:10.3390/rs14041034

37. Xu H. Modification of normalised difference water index (NDWI) to enhance open water features in remotely sensed imagery. Int J Remote Sens. 2006;27: 3025–3033. doi:10.1080/01431160600589179

38. Pawlowicz R, Beardsley B, Lentz S. Classical tidal harmonic analysis including error estimates in MATLAB using T_TIDE. Comput Geosci. 2002;28: 929–937.

39. Roberts DA, Gardner M, Church R, Ustin S, Scheer G, Green RO. Mapping Chaparral in the Santa Monica Mountains Using Multiple Endmember Spectral Mixture Models. Remote Sens Environ. 1998;65: 267–279. doi:10.1016/S0034-4257(98)00037-6

40. Bell TW, Cavanaugh KC, Siegel DA. Remote monitoring of giant kelp biomass and physiological condition: An evaluation of the potential for the Hyperspectral Infrared Imager (HyspIRI) mission. Remote Sens Environ. 2015;167: 218–228. doi:10.1016/j.rse.2015.05.003

41. Pinheiro J, Bates D, Debroy S, Sarkar D. Nlme: linear and nonlinear mixed effects models. R Package Version 3. 2016; 1–127.

42. Di Lorenzo E, Mantua N. Multi-year persistence of the 2014/15 North Pacific marine heatwave. Nat Clim Change. 2016;6: 1042–1047. doi:10.1038/nclimate3082

43. Jacox MG, Alexander MA, Mantua NJ, Scott JD, Hervieux G, Webb RS, et al. Forcing of Multiyear Extreme Ocean Temperatures that Impacted California Current Living Marine Resources in 2016. Bull Am Meteorol Soc. 2018;99: S27–S33. doi:10.1175/BAMS-D-17-0119.1

44. Pimm SL. The complexity and stability of ecosystems. Nature. 1984;307: 321–326. doi:10.1038/307321a0

45. Westman WE. Measuring the Inertia and Resilience of Ecosystems. BioScience. 1978;28: 705–710. doi:10.2307/1307321

46. Morton DN, Bell TW, Anderson TW. Spatial synchrony of amphipods in giant kelp forests. Mar Biol. 2016;163: 32. doi:10.1007/s00227-015-2807-5

47. Fox D, Amend A, Merems A. 1999 Nearshore Rocky Reef Assessment. Oregon Department of Fish and Wildlife Marine Program. 1999. Available: https://www.dfw.state.or.us/MRP/publications/docs/habitat_1999.pdf

48. Fox D, Merems A, Golden J, Amend A. 1996 Kelp/Reef Habitat Assessment. Oregon Department of Fish and Wildlife Marine Program. 1996.

49. Fox D, Merems A, Golden J, Amend A. 1997 Kelp/Reef Habitat Assessment. Oregon Department of Fish and Wildlife Marine Program. 1997.

50. Fox D, Amend A, Merems A, Miller B, Golden J. 1998 Nearshore Rocky Reef Assessment. Oregon Department of Fish and Wildlife Marine Program. 1998. Available: https://www.dfw.state.or.us/MRP/publications/docs/habitat_1998.pdf

51. Merems A. Kelp Canopy and Biomass Survey. Oregon Department of Fish and Wildlife Marine Program. 2011. Available: https://www.dfw.state.or.us/MRP/publications/docs/2011_kelp_report_classicstyle.pdf

52. Edwards MS. Estimating scale-dependency in disturbance impacts: El Ni$\diamond$os and giant kelp forests in the northeast Pacific. Oecologia. 2004;138: 436–447. doi:10.1007/s00442-003-1452-8

53. Edwards MS. Comparing the impacts of four ENSO events on giant kelp (Macrocystis pyrifera) in the northeast Pacific Ocean. ALGAE. 2019;34: 141–151. doi:10.4490/algae.2019.34.5.4

54. Di Lorenzo E, Schneider N, Cobb KM, Franks PJS, Chhak K, Miller AJ, et al. North Pacific Gyre Oscillation links ocean climate and ecosystem change. Geophys Res Lett. 2008;35. doi:10.1029/2007GL032838

55. Parnell PE, Miller EF, Cody CEL, Dayton PK, Carter ML, Stebbinsd TD. The response of giant kelp (Macrocystis pyrifera) in southern California to low-frequency climate forcing. Limnol Oceanogr. 2010;55: 2686–2702. doi:https://doi.org/10.4319/lo.2010.55.6.2686

56. Cavanaugh KC, Siegel DA, Reed DC, Dennison PE. Environmental controls of giant-kelp biomass in the Santa Barbara Channel, California. Mar Ecol Prog Ser. 2011;429: 1–17. doi:10.3354/meps09141

57. Castorani MCN, Bell TW, Walter J, Reuman D, Cavanaugh KC, Sheppard L. Disturbance and nutrients synchronize kelp forests across scales through interacting Moran effects. Ecol Lett. in press.

58. Henson SA, Beaulieu C, Lampitt R. Observing climate change trends in ocean biogeochemistry: when and where. Glob Change Biol. 2016;22: 1561–1571. doi:10.1111/gcb.13152

59. NOAA. 2013-2016 California Sea Lion Unusual Mortality Event in California. 2016. Available: http://www.nmfs.noaa.gov/pr/health/mmume/californiasealions2013.htm

60. Tate HM, Studholme KR, Domalik AD, Drever MC, Romero LM, Gormally BMG, et al. Interannual measures of nutritional stress during a marine heatwave (the Blob) differ between two North Pacific seabird species. Conserv Physiol. 2021;9: coab090. doi:10.1093/conphys/coab090

61. Frischknecht M, Münnich M, Gruber N. Local atmospheric forcing driving an unexpected California Current System response during the 2015–2016 El Niño. Geophys Res Lett. 2017;44: 304–311. doi:10.1002/2016GL071316

62. Arafeh-Dalmau N, Montaño-Moctezuma G, Martínez JA, Beas-Luna R, Schoeman DS, Torres-Moye G. Extreme Marine Heatwaves Alter Kelp Forest Community Near Its Equatorward Distribution Limit. Front Mar Sci. 2019;6: 499. doi:10.3389/fmars.2019.00499

63. Reed D, Washburn L, Rassweiler A, Miller R, Bell T, Harrer S. Extreme warming challenges sentinel status of kelp forests as indicators of climate change. Nat Commun. 2016;7: 13757. doi:10.1038/ncomms13757

64. Mauzole YL, Torres HS, Fu L-L. Patterns and Dynamics of SST Fronts in the California Current System. J Geophys Res Oceans. 2020;125: e2019JC015499. doi:10.1029/2019JC015499

65. Supratya VP, Coleman LJM, Martone PT. Elevated Temperature Affects Phenotypic Plasticity in the Bull Kelp (Nereocystis luetkeana, Phaeophyceae). J Phycol. 2020;56: 1534–1541. doi:10.1111/jpy.13049

66. Zaytsev O, Cervantes-Duarte R, Montante O, Gallegos-Garcia A. Coastal Upwelling Activity on the Pacific Shelf of the Baja California Peninsula. J Oceanogr. 2003;59: 489–502. doi:10.1023/A:1025544700632

67. Malone DP, Davis K, Lonhart SI, Parsons-Field A, Caselle JE, Carr MH. Large-scale, multidecade monitoring data from kelp forest ecosystems in California and Oregon (USA). Ecology. 2022;103: e3630. doi:10.1002/ecy.3630

68. Krumhansl KA, Okamoto DK, Rassweiler A, Novak M, Bolton JJ, Cavanaugh KC, et al. Global patterns of kelp forest change over the past half-century. Proc Natl Acad Sci. 2016;113: 13785–13790. doi:10.1073/pnas.1606102113

69. Filbee-Dexter K, Wernberg T. Rise of Turfs: A New Battlefront for Globally Declining Kelp Forests. BioScience. 2018;68: 64–76. doi:10.1093/biosci/bix147

70. Butler C, Lucieer V, Wotherspoon S, Johnson C. Multi-decadal decline in cover of giant kelp Macrocystis pyrifera at the southern limit of its Australian range. Mar Ecol Prog Ser. 2020;653: 1–18. doi:10.3354/meps13510

71. Smale DA. Impacts of ocean warming on kelp forest ecosystems. New Phytol. 2020;225: 1447–1454. doi:10.1111/nph.16107

72. Ling SD, Johnson CR, Frusher SD, Ridgway KR. Overfishing reduces resilience of kelp beds to climate-driven catastrophic phase shift. Proc Natl Acad Sci. 2009;106: 22341–22345. doi:10.1073/pnas.0907529106

73. Masek JG, Wulder MA, Markham B, McCorkel J, Crawford CJ, Storey J, et al. Landsat 9: Empowering open science and applications through continuity. Remote Sens Environ. 2020;248: 111968. doi:10.1016/j.rse.2020.111968

Supporting information

S1 Fig. Study Domain. Landsat tile composite of the study domain labeled with its corresponding path/row number.

S1 Table. Number of Landsat Images by Year. The number of Landsat images used for each year for each path/row.

S2 Fig. Map of Kelp Canopy Regions. Map of all 10 x 10 km cells labeled by region.

S3 Fig. Latitudinal Trends in Resistance and Resilience. Scatter plots of the a.) resistance and b.) resilience of kelp canopy to the 2014 – 2016 marine heat event compared to the baseline period of 2009 - 2013. Areas dominated by giant kelp are shown in blue and areas dominated by bull kelp are shown in red.

S4 Fig. Mean Canopy Area During and After Marine Heatwave Events. Mean annual canopy area from 2014 – 2021 in 10 x 10 km cells as a percentage of mean annual canopy area from 1984 – 2013. Values of 100% represent kelp canopy areas greater than or equal to the historical mean.

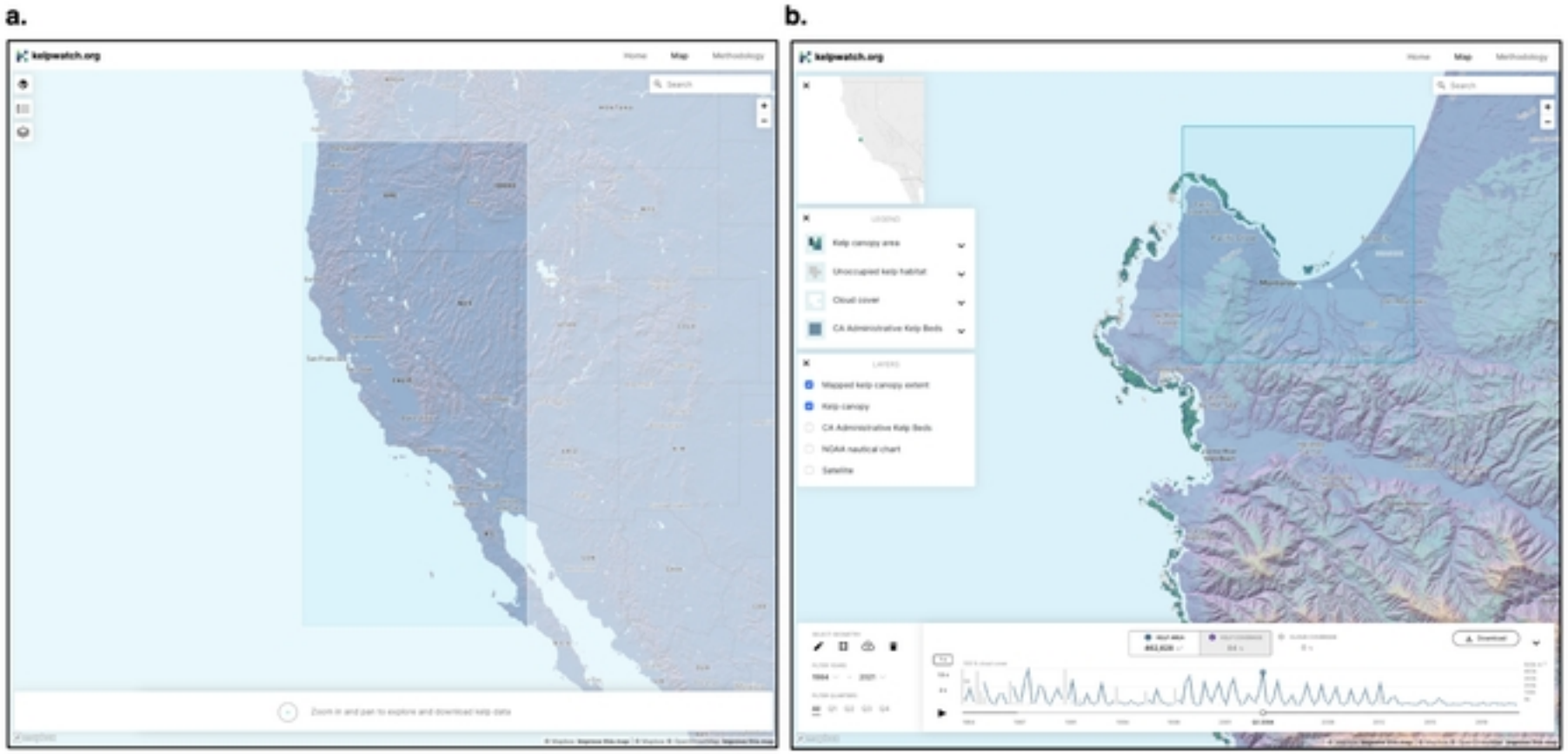
a.
b.
kelpwatch.org
Home
Map
Methodology
Search
Zoom in and pan to explore and download kelp data
LEGEND
Kelp canopy area
Unoccupied kelp habitat
Cloud cover
CA Administrative Kelp Beds
LAYERS
Mapped kelp canopy extent
Kelp canopy
CA Administrative Kelp Beds
NOAA nautical chart
Satellite
Download

Figure 1

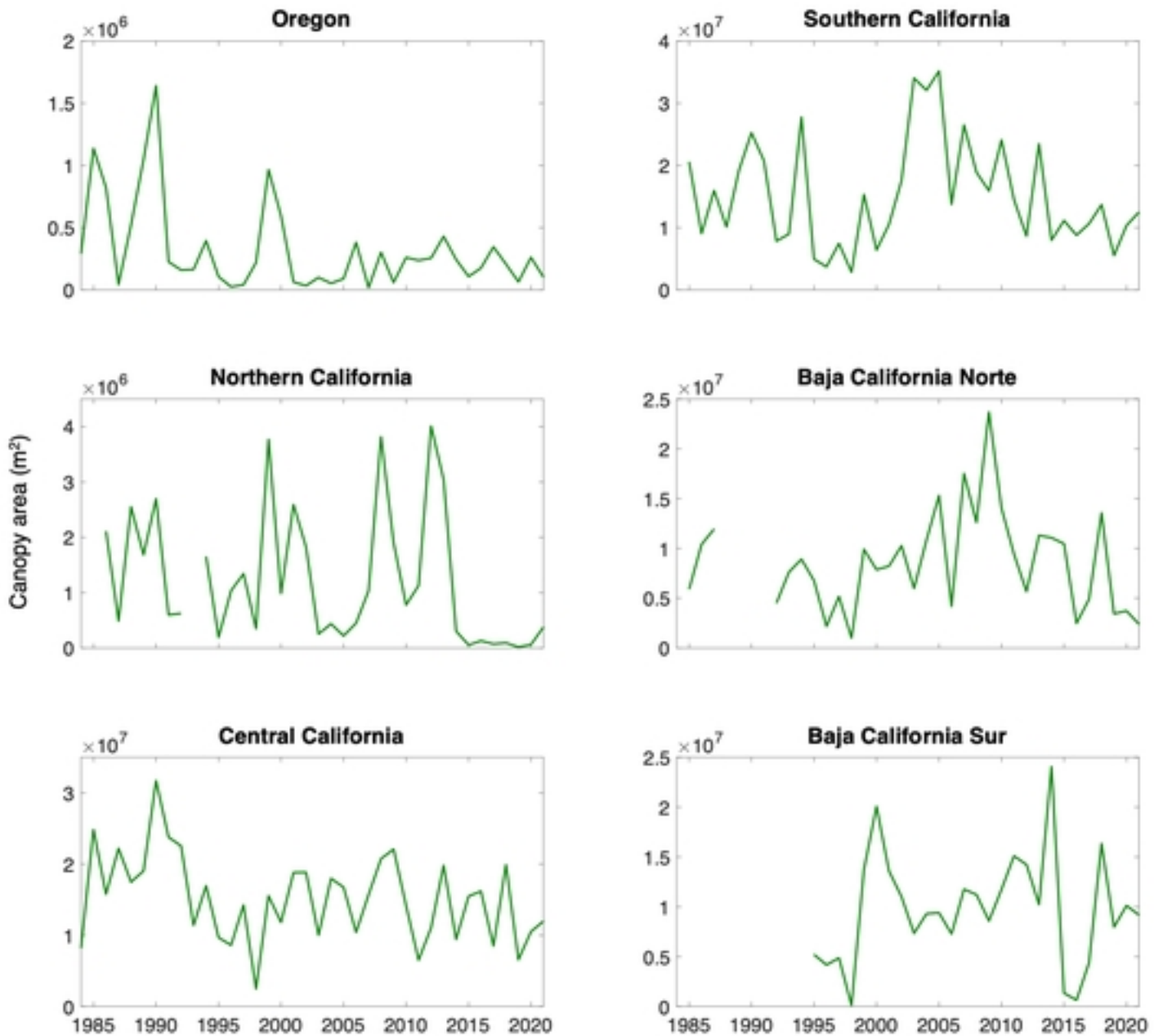
Oregon
Southern California
Northern California
Baja California Norte
Central California
Baja California Sur
Canopy area (m²)
×10^6
×10^7
1985
1990
1995
2000
2005
2010
2015
2020

Figure 2

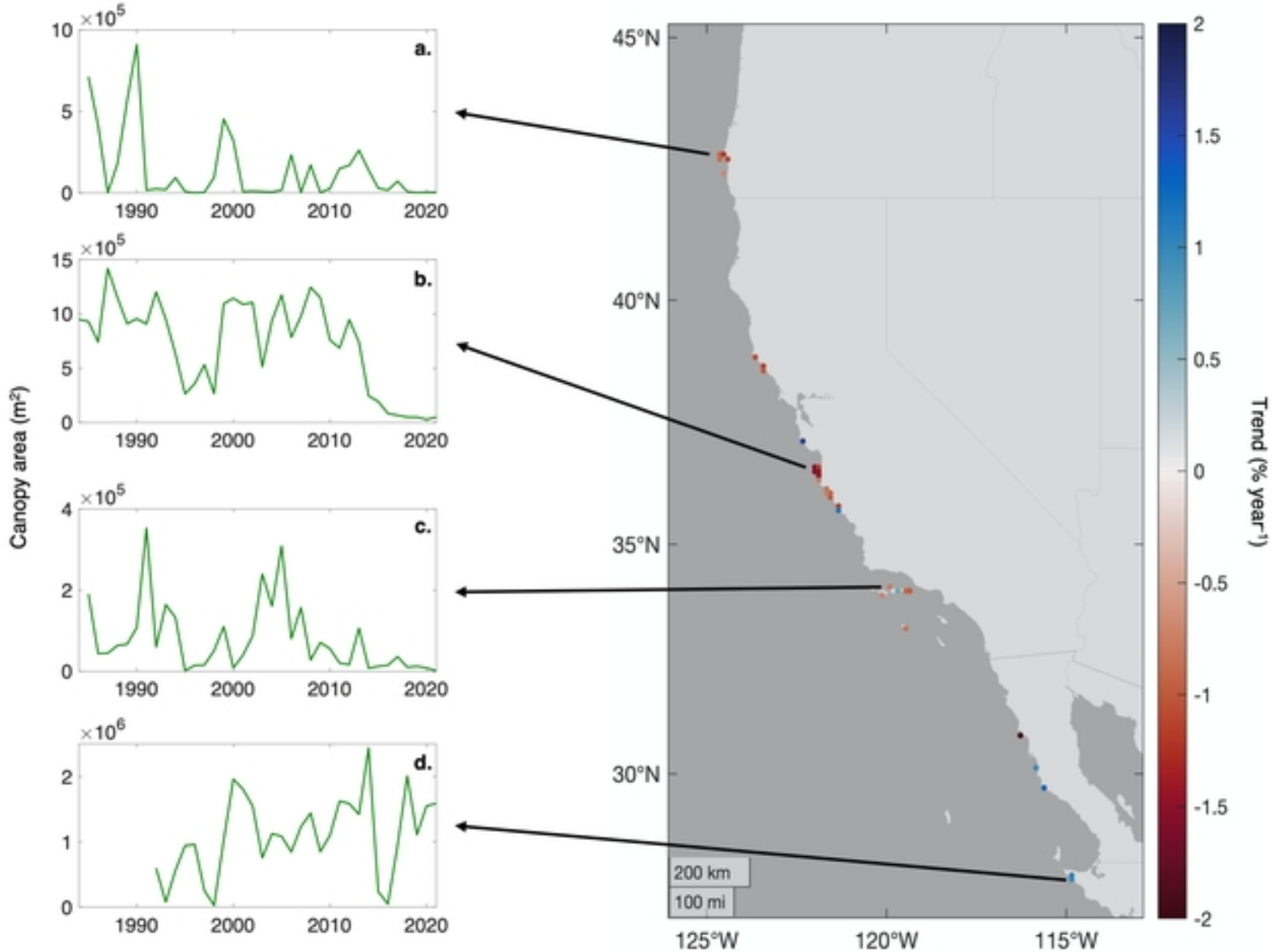
a.
b.
c.
d.
Canopy area (m²)
×10⁵
×10⁶
1990
2000
2010
2020
45°N
40°N
35°N
30°N
125°W
120°W
115°W
200 km
100 mi
Trend (% year⁻¹)
2
1.5
1
0.5
0
-0.5
-1
-1.5
-2

Figure 3

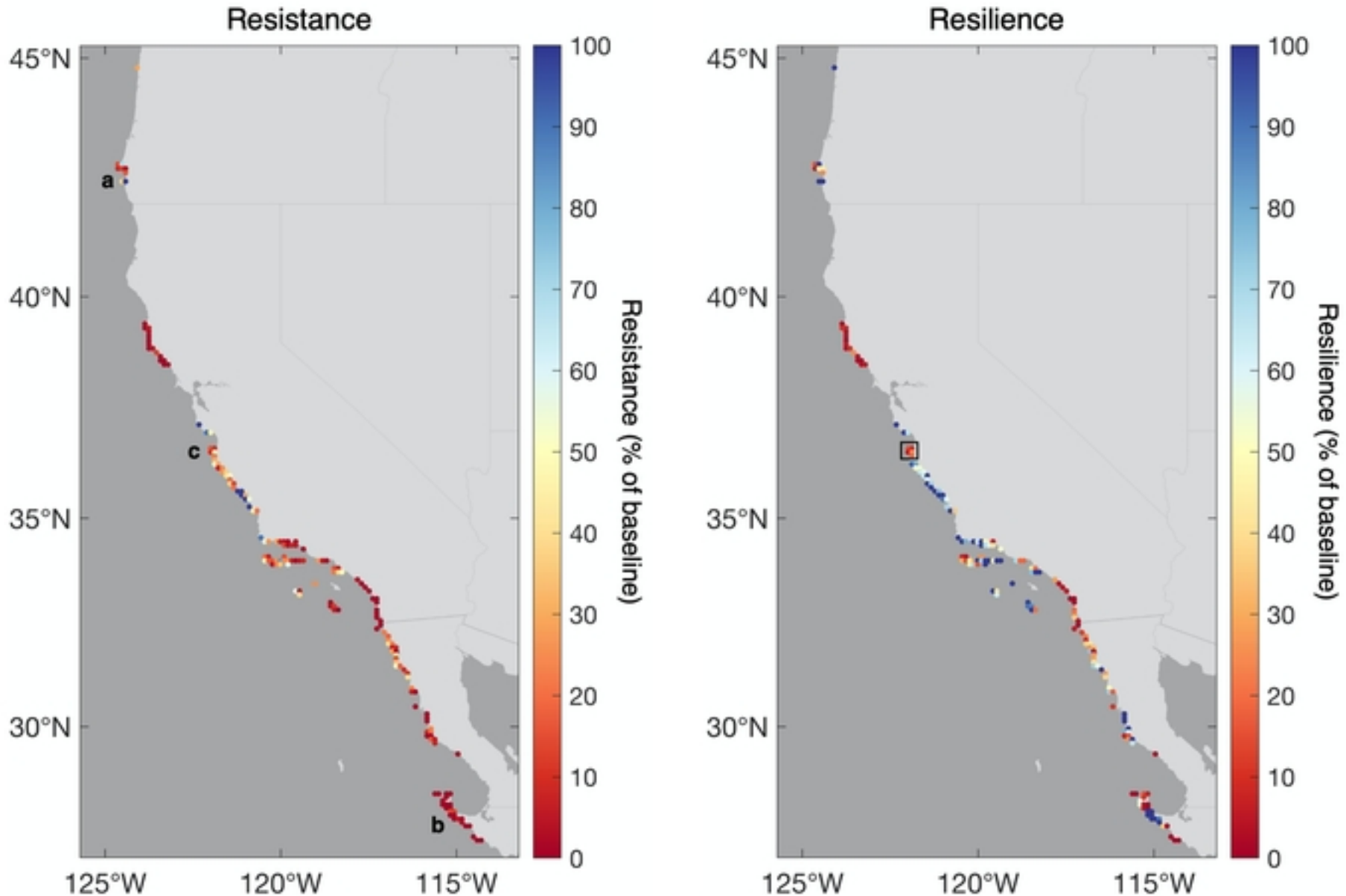
Resistance
Resilience
45°N
40°N
35°N
30°N
125°W
120°W
115°W
a
b
c
100
90
80
70
60
50
40
30
20
10
0
Resistance (% of baseline)
Resilience (% of baseline)

Figure 4

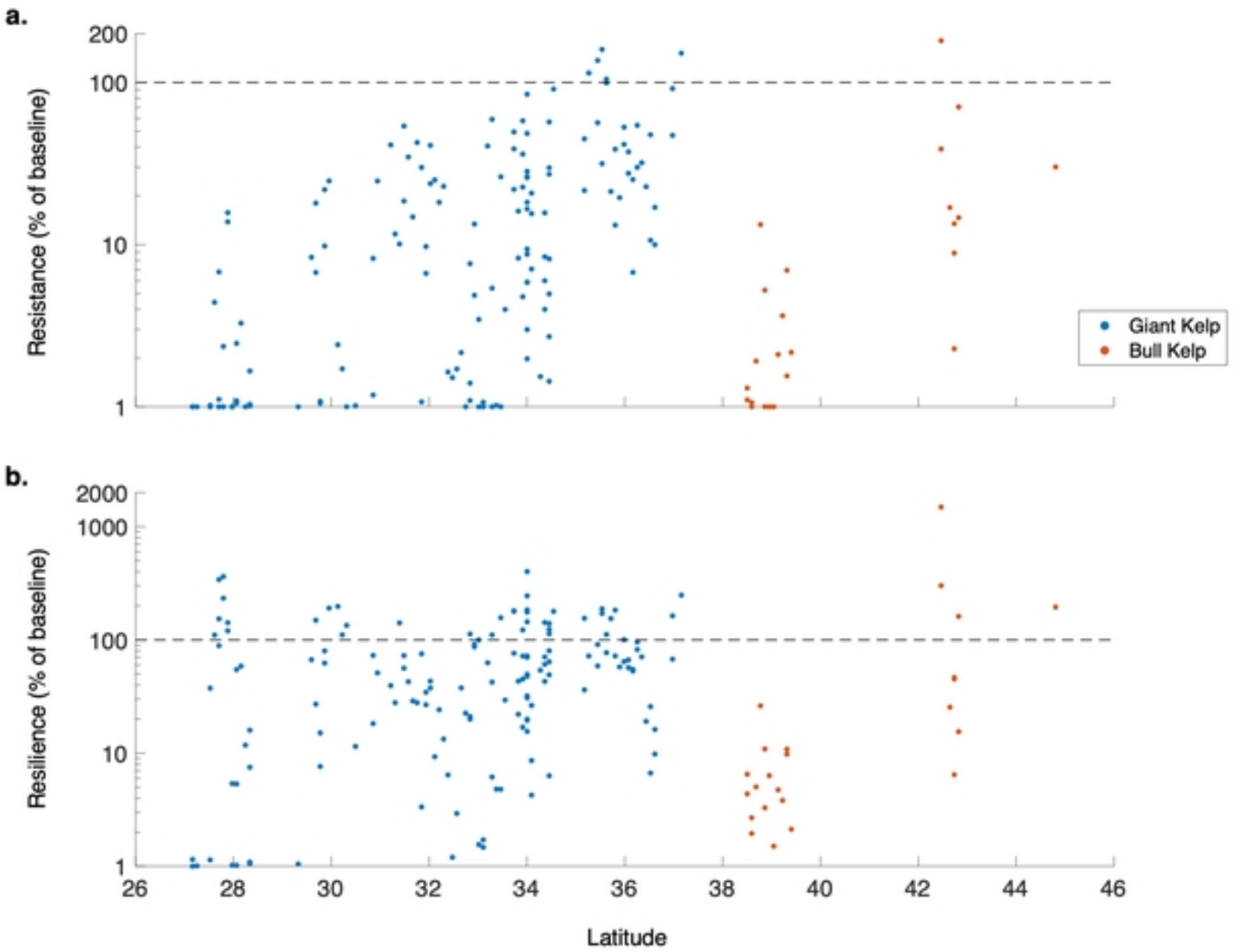
a.
200
100
10
1
Resistance (% of baseline)
Giant Kelp
Bull Kelp
b.
2000
1000
100
10
1
Resilience (% of baseline)
26
28
30
32
34
36
38
40
42
44
46
Latitude

Figure 5

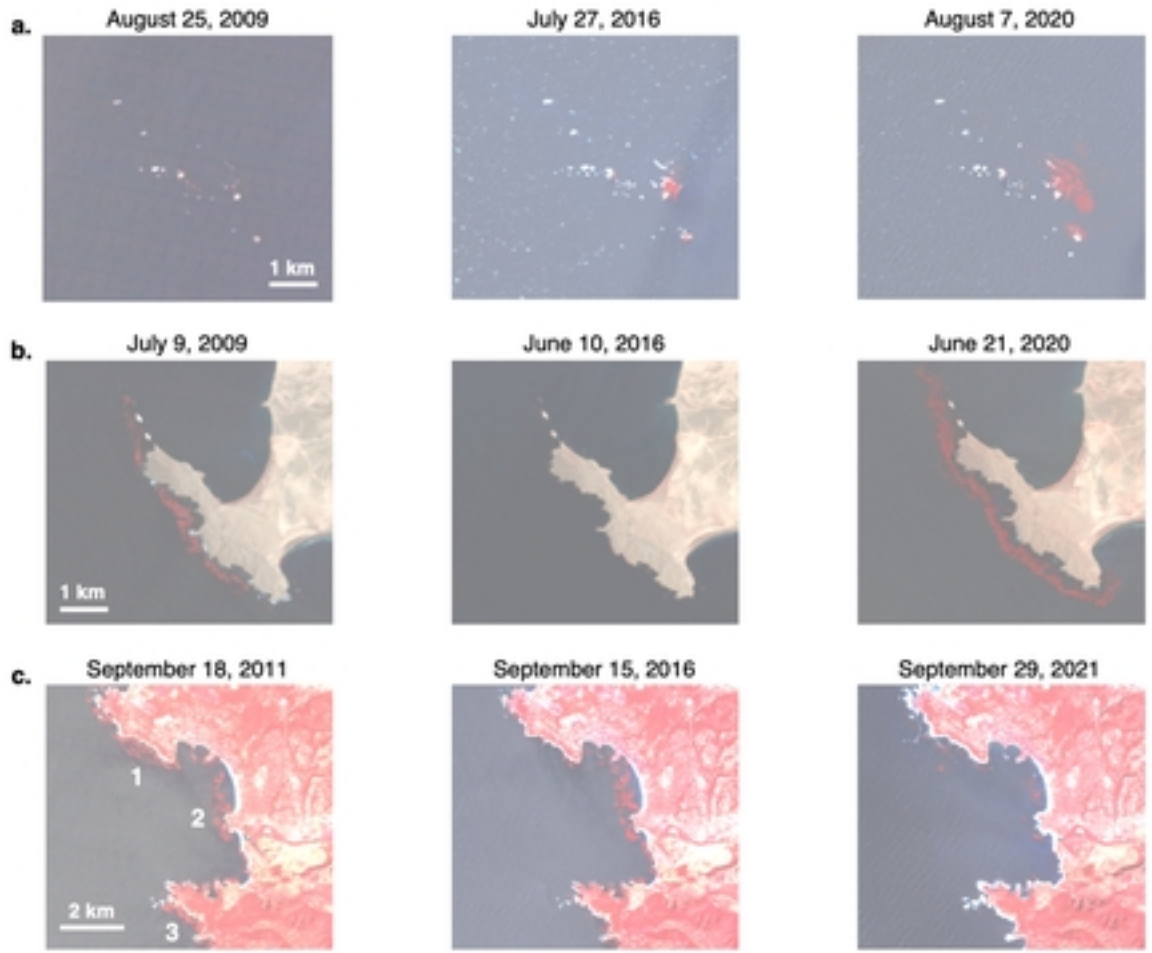
a.
August 25, 2009
July 27, 2016
August 7, 2020
1 km
b.
July 9, 2009
June 10, 2016
June 21, 2020
1 km
c.
September 18, 2011
September 15, 2016
September 29, 2021
1
2
3
2 km

Figure 6

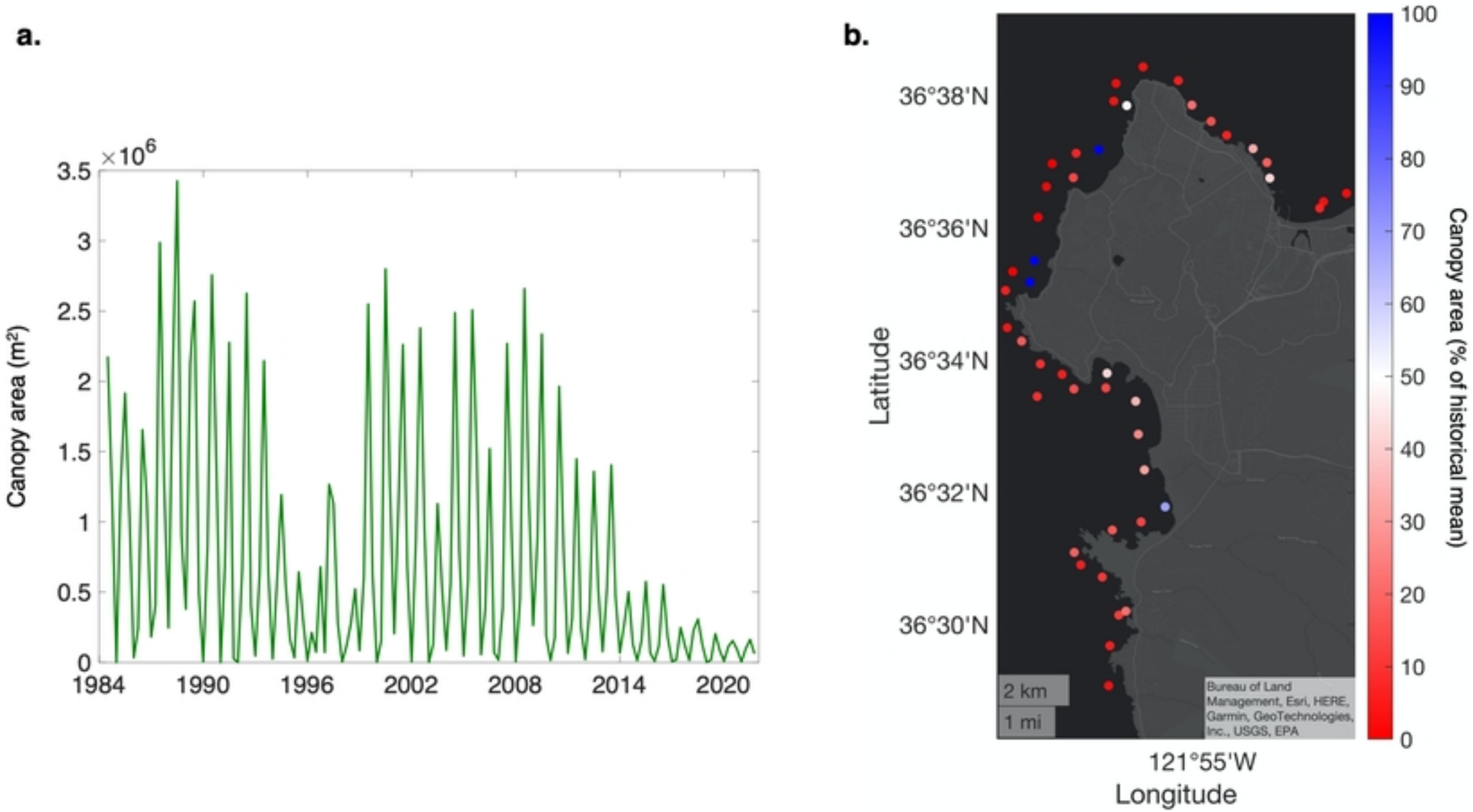
a.
×10^6
3.5
3
2.5
2
1.5
1
0.5
0
Canopy area (m²)
1984
1990
1996
2002
2008
2014
2020
b.
36°38'N
36°36'N
36°34'N
36°32'N
36°30'N
Latitude
121°55'W
Longitude
2 km
1 mi
Bureau of Land Management, Esri, HERE, Garmin, GeoTechnologies, Inc., USGS, EPA
100
90
80
70
60
50
40
30
20
10
0
Canopy area (% of historical mean)

Figure 7